IEEE Access
Multidisciplinary | Rapid Review | Open Access Journal

Received March 15, 2017, accepted March 29, 2017, date of publication April 6, 2017, date of current version May 17, 2017.

Digital Object Identifier 10.1109/ACCESS.2017.2690671

Microwave Breast Phantom Measurement System With Compact Side Slotted Directional Antenna

MOHAMMAD TARIQUL ISLAM[1,2], (Senior Member, IEEE), MD. ZULFIKER MAHMUD[1], NORBAHIAH MISRAN[1], JUN-ICHI TAKADA[3], (Senior Member, IEEE), AND MENGU CHO[2]

[1]Department of Electrical, Electronic and Systems Engineering, Universiti Kebangsaan Malaysia, Malaysia 43600
[2]Kyushu Institute of Technology, Kitakyushu 804-8550, Japan
[3]Tokyo Institute of Technology, Tokyo 152-8550, Japan

Corresponding authors: M. Z. Mahmud (zulfikerm@yahoo.com) and M. T. Islam (tariqul@ukm.edu.my)

This work is supported by the Ministry of Education, Malaysia under the Look East Policy (LEP) Project. Project code: LEP 2.0/14/UKM/TH/01/1.

ABSTRACT In this paper, a new, complete, and comprehensive breast phantom measurement system is presented. A side slotted vivaldi antenna is used for breast phantom measurement. The radiating fins are modified by etching six side slots to enhance the electrical length and produce stronger directive radiation with higher gain. This approach reduces the lower operating frequency and increases the gain and efficiency without compromising the size of the antenna. The overall size of the antenna is 8.8 (L) $\times$ 7.5 (W) cm^2 or approximately 0.4λ $\times$ 0.5λ at the first resonant frequency of 1.79 GHz. The results show that the antenna has a fractional bandwidth of approximately 127% from 1.54 to 7 GHz for return loss less than 10 dB with a directional radiation pattern. The average gain of the proposed prototype is 8.5 dBi, and the radiation efficiency is approximately 92% on average over the operating bandwidth. The fidelity factor for face to face is 0.98, and that for side by side is 0.4479, which proves the directionality and lower distortion of the signal. The prototype is successfully simulated, fabricated, and analyzed. The radiating fins of the proposed prototype are optimized to achieve the desired properties for breast phantom measurement. The antenna is used as the transceiver in a breast phantom measurement system to detect unwanted tumor cells inside the breast. An automated electromechanical imaging system with the necessary data post processing makes it an easy and suitable tool for microwave imaging to detect breast tumors.

INDEX TERMS Microwave imaging, breast phantom measurement, tumor detection, high gain, slotted vivaldi.

I. INTRODUCTION

Over the recent years, Breast cancer reported a prime cause of unwanted death of women all over the world. It is due to the presence of malignant cell inside the breast tissue [1]. Given early breast cancer detection and treatment, the survival rate can even reach 97%, which emphasizes the urgent requirement for a reliable and highly efficient method of early breast cancer detection [2]. For this a new, efficient, nonionizing, low cost, portable and comfortableapproach is highly demanded as a complementary tools to currently used technology of X-ray mammography [3].

Microwave imaging has become one of the most promising candidates for scanning the human body to detect malignant tissues [2]. Microwave imaging systems have the advantages of low cost, high data rate, low complexity and low spectral power density. In an imaging system, the antenna is used as a transceiver to impinge microwave signals on human tissue [4]. The basic principle of microwave imaging is based on the varied electrical properties of different tissues, such as the dielectric constant.

The scatted signal from the antennas reflected from tissues can identify unwanted tumor cells, which have a significantly higher dielectric constant than normal breast tissue [5]–[8]. A circular system with five element antenna array is presented in [9] to scan the entire breast. The system performance is analyzed using S-parameters with realistic anthropomorphic breast phantom without any image re-construction method.

In the breast phantom measurement system, an antenna with a reconfigurable wideband, high gain, and high efficiency is desired. A directional antenna receives a scattered signal from the front target direction, with less effect from interfering signals. Several types of antennas are developed

for breast phantom measurements, such as the unit cell antenna [10], the cross-Vivaldi antenna [11], the compact metamaterials antenna [12] and the slot antenna [13]. The Vivaldi antenna is a valuable tool for microwave imaging in terms of size, bandwidth, high directivity, end fire radiation and low cost [14]. The challenge of designing a Vivaldi antenna is to obtain a directional radiation pattern and resonance at lower frequency. Vivaldi antennas in medical applications have been the subject of research for the last few years [14]. Several researchers have offered different techniques to enhance the performance of Vivaldi antennas [15]. To improve the performance of a Vivaldi antenna, a method based on adding a parasitic ellipse inside the flare is proposed in the literature [16]. The addition of a parasitic ellipse improves the field coupling; however, it does not reduce the size (140×66 mm^2), and it fails to reach lower frequencies. In another study [5], a cavity-backed Vivaldi antenna is proposed for breast phantom measurement. By using Cavity Backed Vivaldi Antenna (CBVA), the size is reduced significantly, whereas the gain does not improve. A square dimension (75×75 mm^2) tapered slot Vivaldi antenna is investigated in [17]. By optimizing antenna parameters, a directive radiation pattern is achieved, but resonance at a higher frequency is not obtained. In [18], an improved Vivaldi antenna with planner directors in front of an aperture and transverse slot is fabricated to increase the gain and directivity. The dimensions of the antenna significantly increase (110×260 mm^2)m and it has a non-contiguous voltage standing wave ratio (VSWR). An antipodal Vivaldi antenna for microwave imaging is reported in [19] with very compact size by metallic bending a feed line structure and modulated Gaussian slot. It has good fractional bandwidth and a wider operating frequency, but the gain and reflection efficiency are less than 5 dBi and 70%, respectively. A number of antennas with different sizes, gains, efficiencies, and reflection coefficients have been recommended for use in medical imaging systems [20]–[22]. Some of them are large, and some of them have a low gain or low radiation efficiency. A planar antenna array that includes 12 corrugated tapered slot elements for use in ultra-wideband (UWB) biomedical microwave imaging systems is presented in [23] to achieve a low profile and moderate gain. However, the performance is achieved at the expense of the antenna being significantly long, with higher dielectric constant. In simulation, the operating bandwidth begins at approximately 5 GHz, which makes it difficult to attain the lower frequency band. The polar Vivaldi antenna proposed in the works [6], [24] achieves microwave imaging while consideringthe conditions of bandwidth, gain and impulse response. However, the presentation is costly in terms of size, where compact dimensions are required.

In this paper, a modified SSVA with enhanced impedance bandwidth for microwave imaging, especially for breast phantom measurement, is presented. Six slots are etched out of the radiating fins to increase the effective electrical length and produce stronger directive radiation. This approach reduces the lower operating frequency limit and increases the gain and efficiency without compromising the size of the antenna. Simulation and measured results show that the proposed antenna can obtain the bandwidth from 1.54 to 7 GHz with an evenly distributed current distribution and a highly directive stable radiation pattern. Simulated and measured results for the reflection coefficient, gain, efficiency, and radiation pattern for different frequencies, as well as the transmitted and received pulse with fidelity factors for dual modes of the antennas, are presented to validate the usefulness of the proposed antenna for a breast phantom measurement system. The proposed antenna has been analyzed and optimized using CST microwave studio software.

Experimental validation of the antenna is completed by developing a breast phantom measurement system to detect unwanted tumor cells inside a breast. For the measurement setup, we use an alternative mechanical approach for collecting data throughout the breast phantom. Two antennas are used for the transmitter and receiver. The antenna is placed stationary at a distance of 18 cm and directly connected to a vector network analyzer (VNA). A breast model is mounted on a stepper motor. The stepper motor is controlled by a PC using microcontroller-based serial communication.

The main objective of this measurement system is to analyze the relationship of the change in backscattered signals from the breast phantom with the change in dielectric properties inside the structure of the phantom. The remarkable variation in the scattered field is an important issue for breast phantom scanners. By using these variations, conclusions can be drawn about whether the system can localize tumor or unwanted cells inside a human breast.

II. ANTENNA DESIGN LAYOUT

The basic goal of this design is to exploit the differences in dielectric constant between healthy and tumorous tissues. The use of multiple resonance frequencies for measurement is necessary for both better resolution and microwave penetration. This is essential for scanning deeper tumors inside the breast with high resolution [5]. For microwave imaging, the antenna should have high gain, wide bandwidth, resonance at a lower frequency, and higher directivity. Vivaldi antennas fulfill these requirements because of their high directive nature with high gain due to their tapered slot design and they have a high peak value for the pulse envelope. Vivaldi antennas also offer stable group delay and allow for a narrow pulse width. To achieve these desired characteristics, a conventional Vivaldi antenna has been customized with the introduction of the SSVA [6], [25], [26]. The geometric layout and fabricated prototype of the proposed antenna are shown in Figure 1. The antenna is printed on a Rogers RT/duroid 5870 substrate with a thickness of 1.57 mm, relative permittivity of 2.33 and loss tangent of 0.0012. The overall size of the antenna is 8.8 (L) $\times$ 7.5(W) cm^2 or approximately $0.4\lambda \times 0.5\lambda$ at 1.79 GHz, which is the first resonant frequency. The radiating properties of the SSVA are determined by a set of exponential curves, the tapered rate, the cavity structure, the slot line, the back wall offset, the stub arrangement, the feeding position,

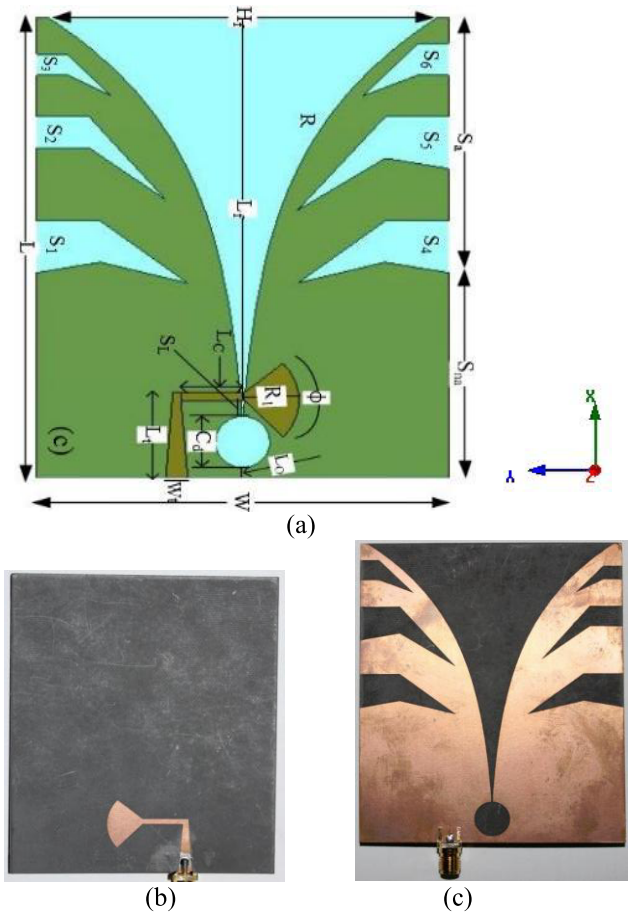

FIGURE 1. The proposed antenna (a) Geometric Layout b) Front Side (radiating fins) c) Back side.

and the structure of the radiating fins. By etching slots, all these parameters are adjusted, and the radiating fins are modified. Irregular slots are implemented to increase the electrical length, especially to reduce the lower operating band. The main radiating lobe is its flare, with height $H_f = 7.09$ cm and length $L_f = 7$ cm with a taper rate of $R = 0.04$ (factor determining the opening rate of the flare) of the inner exponential profile. The exponential curve that employs the Vivaldi antenna is defined as:

$$x = C_1 e^{Rz} + C_2 \tag{1}$$

Where $C_1 = \frac{x_2 - x_1}{(e^{Rz_2} - e^{Rz_1})}$ and $C_2 = \frac{x_1 e^{Rz_2} - x_2 e^{Rz_1}}{(e^{Rz_2} - e^{Rz_1})}$

The points (x_1, z_1) and (x_2, z_2) are the end points of the flare. There has a cavity at the end of the flare with diameter $C_d = 10.3$ mm. The cavity is adjusted with the equation:

$$C_a = 0.5C_d - 0.5C_d(\cos\theta) \tag{2}$$

Where $\theta = \sin(\frac{S_w}{C_d})$

The cut-off frequency of the proposed SSVA with the present dimensions can be calculated using the equation described in [27]:

$$f_c = \frac{c}{\left[w'\sqrt{(\varepsilon_r)}\right]} \tag{3}$$

Here, c is the speed of light, f_r is the resonant frequency, ε_r is the relative permittivity of the antenna material, and w' is the width of the opening of the flare edge.

There is a slot line (S_L) between the cavity and flare with a length of 1.5 mm and a width of 0.5 mm. The value of the back wall offset (L_O) is 1.6 mm. The total conductor is divided into two regions, the slotted and non-slotted areas. The ratio of the slotted to non-slotted area is 46:44. The lower slots (S_1, S_2, and S_3) vary as the higher order slots are decreased by 2 mm in gap and height. The upper slots S_4 and S_5 are symmetric, but the latter is decreased by 4 mm. To achieve a larger operating bandwidth, a microstrip slot with a radial stub is introduced. The stub begins at 45°, with a total coverage stub-angle of $\varphi = 90°$ and a radius of $R_1 = 10$ mm. There is a microstrip taper with length $L_t = 15.6$ mm and starting width $W_t = 4$, which is decreased with the taper factor of 0.04. The microstrip coupler is placed between the microstrip taper and stub. The length of the coupler is $L_C = 12$ mm, and the width is 1.5 mm. The distance from the cavity to the center of the microstrip coupler, marked as the microstrip coupler inset, is approximately 3.757 mm. A 50Ω SMA connector is used to feed the antenna connected to the microstrip tapered line. The SMA connector has a 2.08 dielectric constant and 4.62×10^4 S/m electrical conductivity.

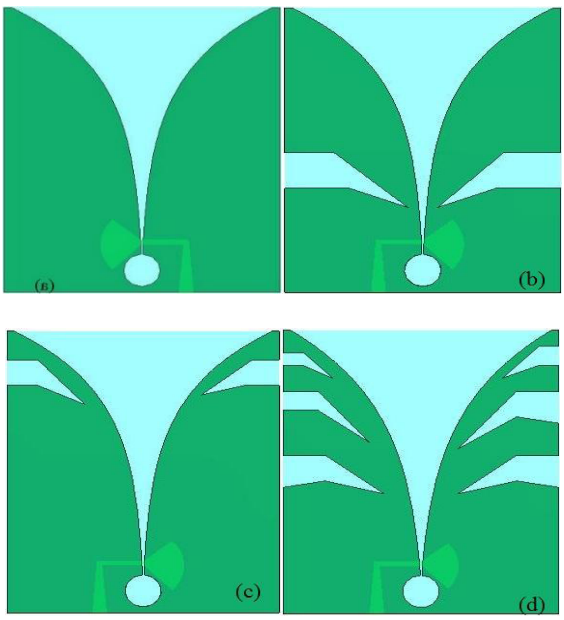

FIGURE 2. The proposed antenna (a) Without slot (b) With lower slot (c) With Upper slot (d) With six slot (Proposed).

III. PARAMETRIC STUDY

Figure 2 shows the evolution of the proposed antenna. The effects of the slots in the radiating fins on the S_{11}, gain and efficiency are shown in Figure 3. Table 1 shows the comparisons of the effects of the slots on antenna performance, which are found in Figure 3. It is clearly seen that the proposed prototypes provide a wider bandwidth than those

TABLE 1. Comparisons of the slot effects on the reflection coefficient S_{11}.

Antenna Structure	Operating Frequency (S_{11}<-10dB) GHz	Peak Gain(dBi)	Average Efficiency(%)
Without Slot	1.82-6.3 (Excluding 3.4-3.8 GHz)	9 dBi	85%
With Lower Slot	1.65-6.3(Excluding 3.55-3.70 GHz)	8.9 dBi	86%
With Upper Slot	1.8-6.1(with Band gap 2.15-2.47 GHz)	8.95 dBi	87%
Proposed	1.54-7 GHz	9.8 dBi	92%

without any slots, a lower slot or an upper slot. The Vivaldi antennas without slots have a return loss higher than 10 dB from 1.82 to 6.3 GHz, with a band gap from 3.4 to 3.8 GHz. Using the lower slot, the lower frequency is shifted to 1.65 GHz but shows a band gap from 3.55 to 3.70 GHz. By using the upper slot, the lower frequency rises to 1.8 GHz, and the upper frequency becomes 6.1 GHz, with a gap of 2.15-2.47 GHz. By using the proposed configuration, the lower operating frequency shifted to 1.54 GHz, and the upper limit reached 7 GHz with a contiguous wideband operating frequency. The peak gain of the proposed structure is 9.8 dBi, whereas 9, 8.9 and 8.95 dBi are those for without a slot, with a lower slot, and with an upper slot, respectively. The gain is increased significantly at lower frequencies due to the modification of the radiating fins. Slots on the radiating fins enhance the electrical length and produce stronger directive radiation due to suppression of unwanted surface currents that radiate vertically with theend-fire direction at the outer edge of the radiation arms. It remarkably affects the gain and efficiency. The efficiency of the proposed structure is stable and more than 5% improved over those of other structures.

IV. ANTENNA PERFORMANCE MEASUREMENT

The performance of the proposed antenna has been analyzed and optimized using CST microwave studio. Simulation results are plotted using thescientific graphing and data analysis software Origin Pro. The measured results were obtained using the Agilent E8362C vector network analyzer that covers the range of 10 MHz to 67 GHz and theSatimo near field measurement lab (UKM StarLab) using Satimo passive measurement (SPM) and SatEnv software. The measurement setup is shown in Figure 4(d).The simulated and measured reflection coefficients (S_{11}) of the antenna are shown in Figure 4(a). The-10 dB operating bandwidth of the SSVA is approximately 5.46 GHz, starting from 1.54 GHz to 7 GHz. The first resonance is found at 1.79 GHz, the second higher resonance is at 2.89 GHz and the highest resonance is at 5.81 GHz. The lower frequency bandwidth is significantly affected by the used slots in the radiating fins. The measured and simulated results have very good agreement and even the resonance points are sharply matched. Though the design of the proposed antenna is very simple and compact in size, it achieves a much wider bandwidth compared with recently published antennas in the literature [3], [10]–[12], [19]–[21].

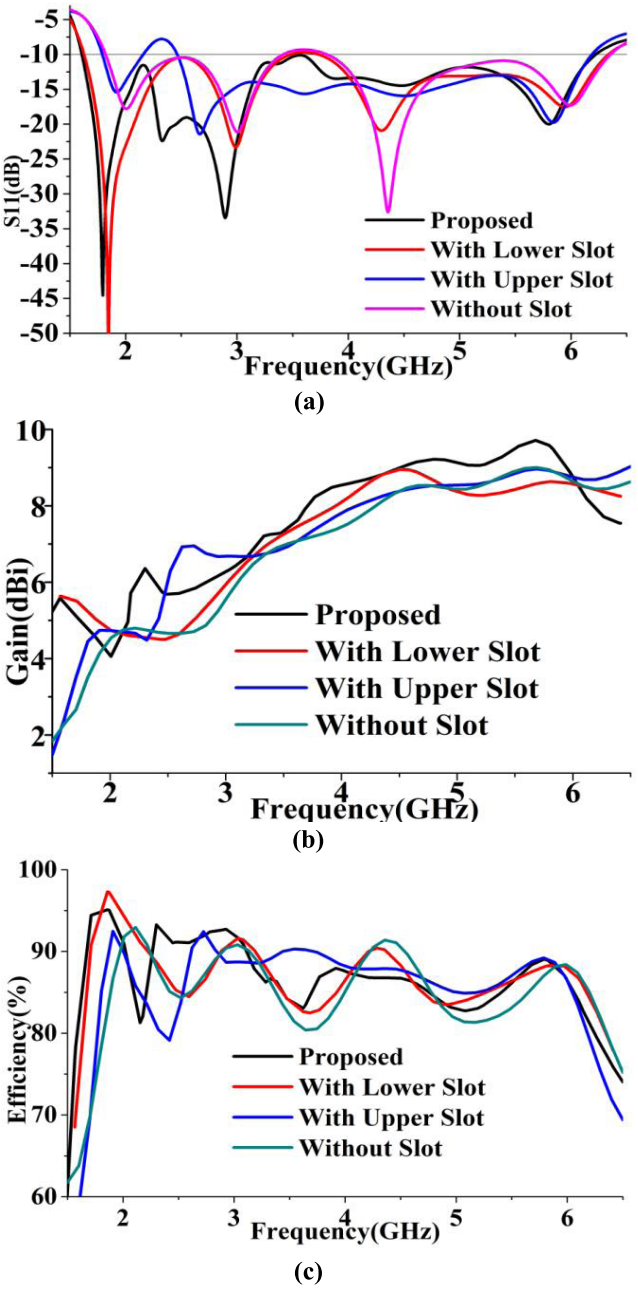

FIGURE 3. Effect of the slots on the radiating fins to (a) The S_{11} (b) The Gain and (c) The efficiency of the proposed antenna.

One major finding of this study is that there is no gap or mismatch in the entire bandwidth.

Figure 4(b) shows the measured and simulated gain against frequency. The minimum and maximum gain over the operating bandwidth is 4 and 9.8 dBi, respectively, with a smart average of 8.5 dBi. Again, the simulated and measured results are in good agreement. The SSVA offers a simple structure and compact dimensions, and it is light weight compared to other antennas, while the peak gain increased approximately 1 dB over recently published antennas. Figure 4(c) illustrates the measured and simulated efficiency over the bandwidth. The efficiency is calculated using the real and imaginary

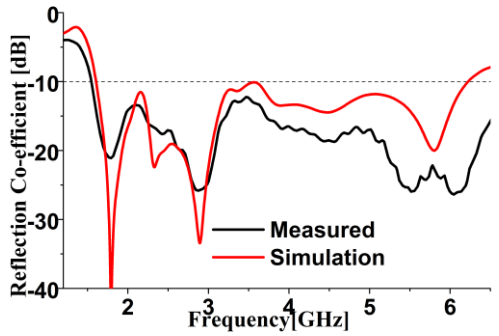

(a)

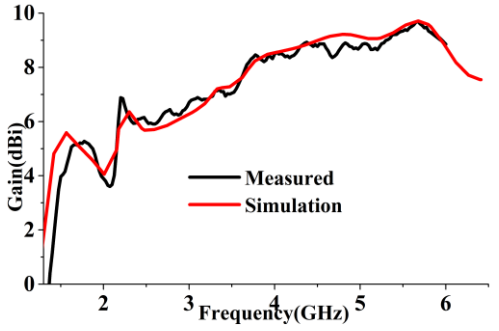

(b)

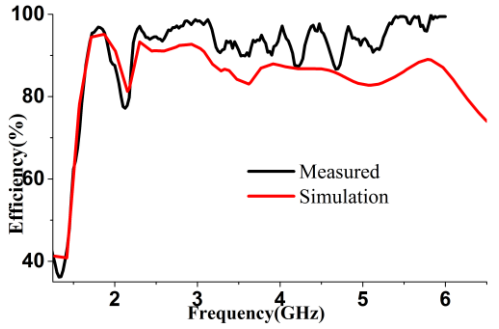

(c)

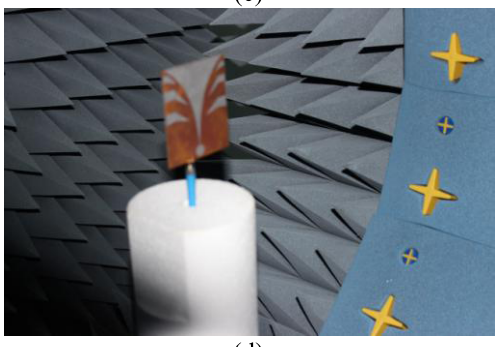

(d)

FIGURE 4. **Antenna Performance (a) Reflection-coefficient (b) Gain (c) Efficiency (d) Satimo Setup.**

layers of a sphere using the two axes φ and θ. The data is computed according to the following formula:

$$Efficiency = \frac{\int |sin\theta_i| \int \left(R_1^2 + I_1^2 + R_2^2 + I_2^2\right)}{4\pi} \quad (4)$$

Where, θ_i is the position along second axes.

The average radiation efficiency is approximately 92% over the bandwidth, with a minimum of 85% and maximum of 97%. The efficiency is almost 5-10% more than the evolution structures of the proposed antenna. The simulated and measured radiation patterns at resonant frequencies are plotted in Figure 5. The 3D view overthe same frequencies is also present. In the Satimo measurement lab (UKM StarLab),the antenna is measured according to Phi axis rolling and Theta stepping. The measurements are logged in tables of Theta and Phi spherical coordinates. The spherical coordinates relate to the Cartesian axes as follows: the XZ Cut is Theta=0 to 360 & Phi=0, theYZ Cut is Theta=0 to 360 & Phi=90 and the XY Cut is Theta=90 & Phi=0 to 360. The xz-plane ($\varphi = 0$) and yz-plane ($\varphi = 90$) are considered as the E-plane and the H-plane, respectively.According to the near field performance, the proposed antenna is unidirectional, and the direction of the main beam is towards the boresight. Over the operating frequency band, the main lobes of the radiation patterns are fixed in the end-fire direction (x-axis direction). Stable radiation directivity is achieved that ensures a higher range of the scattered signal with low unwanted noise from the backward direction. The directivity is increased with increasing frequency because the radiating element is excited with higher order modes [28]–[30] that typically result in a directional radiation pattern.

In Figure 6, the surface current distribution is shown at thefrequencies of 1.79, 2.89 and 5.81 GHz. The main current conducting area is on theradiating fins and around the cavity. At lower frequency, the current is mostly distributed around the microstrip taper, coupler and stub. At higher frequencies, a few nulls are observed due to the excitation of thehigher order current mode. The slots on the radiating fins change the current path and create higher order current modes. For this, remarkable changes in the antenna characteristics are found. By adding slots, simultaneously, the side lobe levels are reduced, the gain in the main lobe is increased and the squint effect is corrected, providing improvement in radiation characteristics. The slots promote the optimal conditions for the main radiator to avoid trapping. The radiation characteristics are improved by the slot edges due to control of the current distribution near the lateral antenna edges. The secondary current distributions are concentrated at the side edge, leading to high radiation.

The form of the output signal at the receiving antenna is the convolution of the input signal and the impulse response. The time domain performances of the antenna when it operates face to face and side by side at a distance of 200 mm are shown in Figure 7(a &b). When two antennas are placed face to face the transmitted and received waveforms are the same in all cases. In the face to face orientation, the antennas are capable of radiating short pulses with very small distortion and minimal late time ringing. Only the pulse has spread slightly. In the side by side orientation, the transmitted and received waveforms are not exactly the same. Due to the directional characteristics of the antenna, the transmitted signal is spread in a single direction. For this, the transmitted

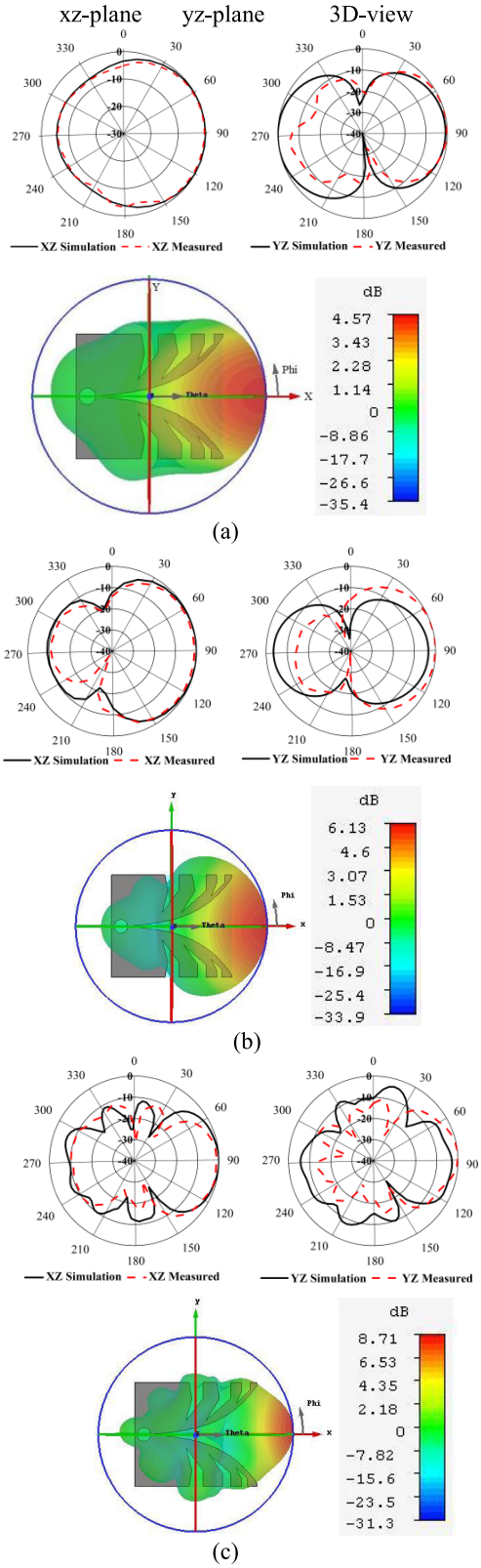

FIGURE 5. Simulated and measured 2D and 3D radiation pattern view at (a) 1.79 GHz (b) 2.89 GHz (c) 5.81 GHz.

and received signals are not the same shape. The fidelity is the highest magnitude of the cross-correlation between the transmitted and received pulses. If τ is the transmission

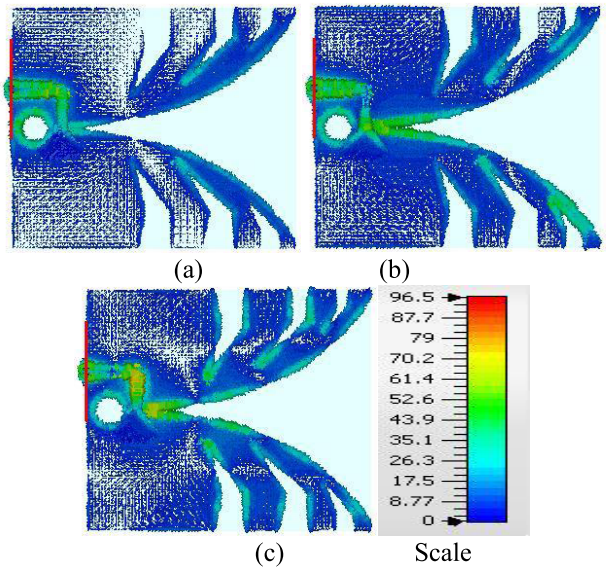

FIGURE 6. Surface current distribution at (a) 1.79 (b) 2.89 and (c) 5.81 GHz.

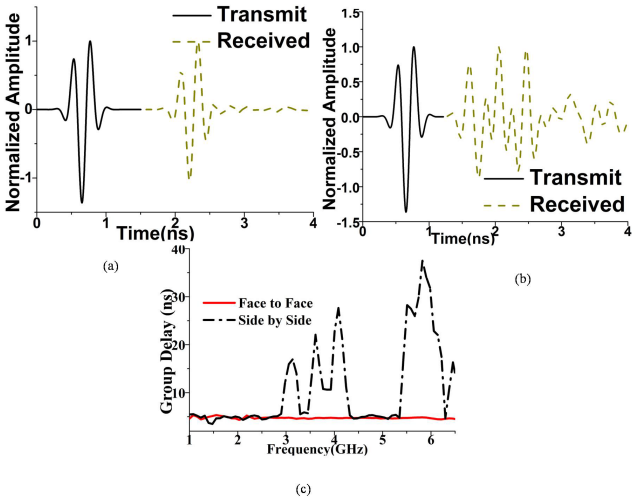

FIGURE 7. Transmitted and received pulses (a) face to face and (b) side by side (c) Group delay.

delay, then, the correlation factor is defined by the following equation:

$$F = \max \frac{\int_{-\infty}^{+\infty} x(t)y(t-\tau)dt}{\sqrt{\int_{-\infty}^{+\infty} |x(t)^2| dt \int_{-\infty}^{+\infty} |y(t)^2| dt}} \quad (5)$$

Where the transmitted (TX) and received (RX) signalsare represented as x (t) and y (t), respectively.Matlab is used to implement the fidelity equation and calculate its value. In the face to face orientation, the fidelity factor is 0.98, whereas in the side by side orientation, it is 0.4479. The fidelity factor of the proposed antenna is higher than those of recently published Vivaldi antennas. A higher value forthe fidelity factor guarantees a lower distortion inthe transmitted

TABLE 2. Comparison of proposed SSVA to literature.

Ref. No	Dimension (mm)	Starting Frequency	Maximum Realized Gain (dBi)
[5]	63×51	2.5 GHz	9.7
[16]	140×66	2 GHz	9.4
[18]	260×110	2.4 GHz	10.4
[16]	126×153	2.65	11
[25]	60×60	1.8 GHz	7.8
[32]	112×40	3.4 GHz	7.4
[33]	60×60	2.4 GHz	7.9
[34]	135×100	3.1 GHz	Not reported
Proposed	88×75	1.54 GHz	9.8

signal. These attributes confirm that the antenna is suitable for microwave imaging.

Group delay represents the phase distortion of the signals. It is obtained as the negative derivative of the phase response with respect to frequency. In the side by side orientation, the group delay is higher than that in the face to face orientation. In the face to face orientation, it is nearly constant over the bandwidth. For this reason, the antenna is recommended to be used in the face to face orientation for microwave imaging.

Table 2 lists the comparisons between the proposed antenna and antennas from the literature. The proposed SSVA is smaller in dimensions than the Vivaldi configurations reported in [3], [10]–[12], [19]–[21], and that makes it suitable for microwave imaging applications that require directional properties.

V. IMAGING SYSTEM DESIGN

The desired goal of breast phantom measurement is to correlate the change inthe backscattering signal with the presence of some high dielectric inclusion, such as a tumor. In this work, we have developed an automated microwave imaging system. The block diagram of the imaging system is depicted in Figure 8(a). All the devices and electromechanical circuits are controlled by a single PC. Antennas are used as the transceiver, and the scattering signal is collected using a vector network analyzer (VNA). For the measurement setup, we use an alternative mechanical approach for collecting data throughout the breast phantom. The mechanical rotation platform can rotate in polar coordinates from 0 to 2π. An Arduino Uno circuit is used to control the rotation platform using a stepper motor. Total 360° rotation is performed, with measurement at 120 equivalent points with 3° separation. We don't use any human body or patient in this case due to the safety permission which is ongoing. For laboratory tests, we rotate the phantom to collect data throughout the phantom to locate the position of the tumor. In the resulting system, the rotation platform will be set up and work as a medical imaging bra that will rotate clockwise. We use a homogeneous breast phantom with a single tumor that has a higher dielectric constant, a concept from [10], for testing the system. A commercially available off-the-shelf breast phantom developed in Japan with the prerequisite criteria, as shown in Figure 8 (b), is used. The size of the phantom is approximately 16×8 cm^2, with the standard dielectric constant of a human breast and a target tumor of 10 mm diameter inside. The phantom contains four layers, namely, the skin layer, the breast tissue layer or fat, the tumor and the normal air layer. The skin layer has the following properties: dielectric constant = 38, thickness = 2.5 mm, and conductivity = 1.49 S/m. The breast tissue layer has a maximum width of 8.75 cm, with conductivity = 0.141 S/m and dielectric constant = 5.14. The tumor has dielectric constant = 67 [33], [34]. Tumorous cells normally have a high water content and a dielectric constant that is higher than that of low water tissues, such as fat [35], [36].The proposed antennas are placed face to face at a distance of 18 cm, and each of them is 6.5 mm from the breast skin layer. The breast phantom is placed on the rotation platform, and two antennas are placed beside the phantom and are connected to the VNA (Agilent N5227A). The VNA is connected to a PC via a GPIB port, and data are transmitted to PC through this setup. The experimental setup is shown in Figure 8(c). Finally, the effects of the normal breast tissue and tumor on both forward and backscattering signals are studied and processed.

VI. IMAGING RESULTS

In measurement, we test the antenna performance to detect the tumorous cells inside the breast. For experimental measurement, the VNA parameters are set with a bandwidth of 10 Hz,the number of points is M=201, and the 1.54 to 7 GHz frequency range is covered. The VNA is connected to a PC via a GPIB port, and data are received for further processing. By using the experimental setup, the complex frequency domain S-parameter $\Gamma\,(\varphi_n, f_m)$ data are captured, where m=1,2,...M, and n=1,2.....N, represent the angular positions of each rotation. The transmitted parameters depend on the entire path between the two antennas, where the tumor crosses twice during the complete rotation. The reflected signals mostly represent the shallow depths under the skin layer because signals that are reflected off the opposite side of the breast phantom have to travel through the phantom twice and are significantly attenuated. Thus, antennas with very low inherent return loss are ideal to detect weak reflected signals. The collected data is post-processed, and the image of the breast interior is reconstructed. Inverse discrete Fourier transform is used to convert the reflection co-efficient from the frequency domain to the time domain for each antenna.

$$S\,(\varphi_n, t_k) = exp\,\{[D_{k\times m}]\} \times \Gamma\,(\varphi_n, f_m) = \begin{bmatrix} S\,(\phi_1, t_1) & \dots & S\,(\phi_N, t_1) \\ \vdots & \ddots & \vdots \\ S\,(\phi_1, t_m) & \dots & S\,(\phi_N, t_k) \end{bmatrix} \quad (6)$$

Where

$$f_m = f_1 + (m-1)(f_h - f_1)/(M-1) \quad (7)$$

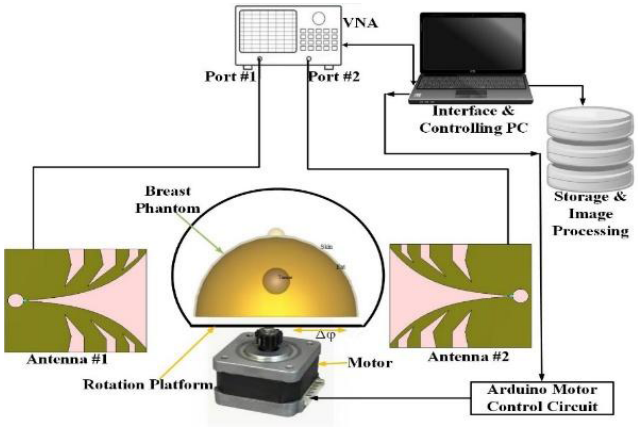

(a)

(b)

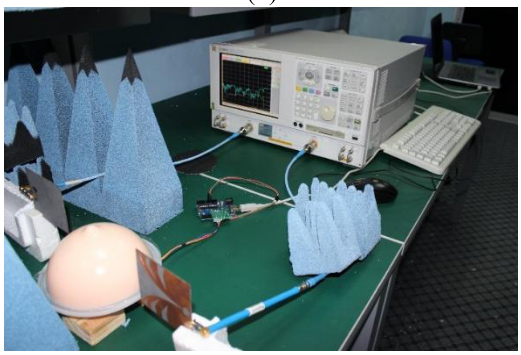

(c)

FIGURE 8. (a) Block diagram of imaging system (b) Breast phantom (c) Experimental setup.

$$\Gamma(\varphi_n, f_m) = \begin{bmatrix} \Gamma(\phi_1, f_1) & \cdots & \Gamma(\phi_N, f_1) \\ \vdots & \ddots & \vdots \\ \Gamma(\phi_1, f_M) & \cdots & \Gamma(\phi_N, f_M) \end{bmatrix} \quad (8)$$

And

$$[D_{k\times m}] = \begin{bmatrix} j\omega_1 t_1 & \cdots & j\omega_m t_1 \\ \vdots & \ddots & \vdots \\ j\omega_1 t_m & \cdots & j\omega_m t_k \end{bmatrix} \quad (9)$$

ω_m is angular velocity and k is the equidistance points.

The time domain image is characterized by its intensity distribution I. The system is linear and space invariant. The inversion schemes model is used for image processing:

$$I(x, y) = O(x, y) * p(x, y) \quad (10)$$

Where O is the object, $*$ is the two-dimensional convolution operator and p is the point spread function (PSF) a spatial impulse response. The $p(x, y)$ is given as:

$$p(x, y) = \frac{i\omega\rho\vartheta_o}{4\pi^2} H(z_o, x, y) \frac{\partial}{\partial z} H(z, x, y)_{z=z_o} \quad (11)$$

Where

$$H(z, x, y) = \frac{i2a}{k} \int_0^{\pi} d\varphi \frac{scos\varphi - a}{s^2 + a^2 - 2ascos\varphi}$$

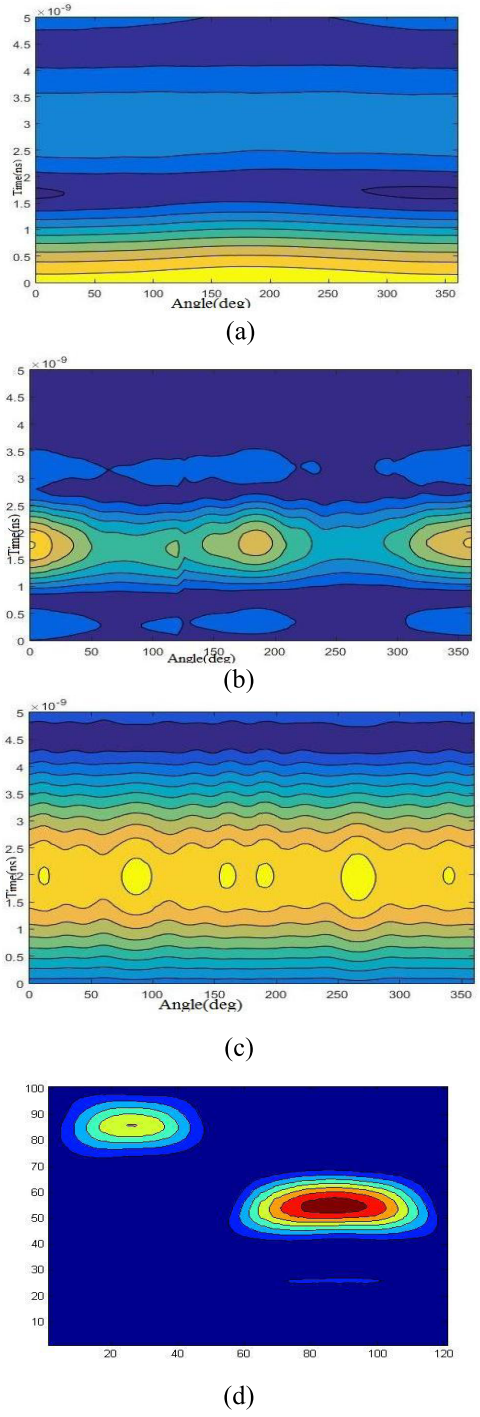

(a)

(b)

(c)

(d)

FIGURE 9. Imaging result (a) Without tumor (b) with tumor at 0° positions (c) with tumor at 90° (d) After post process.

$$\times \left(e^{-ik\sqrt{s^2+a^2-2ascos\varphi+z^2}} - e^{-ikz} \right) \quad (12)$$

$s^2 = x^2 + y^2$, a is the radius of the transducer area, ϑ_o is the velocity amplitude and ρ is the density of the medium. Here, the blind-deconvolution method is used, where the PSF is optimized using the latest heuristic optimization algorithms [37]. The tumor is clearly detected by differentiating the collected scattering signals from healthy and unhealthy tissuesin the breast phantom.

It can be noted that in the image generated from reflected S-parameters in Figure 9, the tumor is visible near 350°. The variation appears twice in the transmitted S-parameter with another slightly lower power artifact at approximately 170°. The transmitted parameters rely on the entire path between the two antennas, which the tumor crosses twice during the complete rotation. The artifacts appear after 1.75 ns. This can be translated into the distance from the antenna using the propagation rates in the different media involved.

The performances of the proposed antenna and imaging system are better than those of the previously proposed Vivaldi antenna and imaging systems. Some of those studies present only simulation results [10], [12], and other systems have deficient imaging performance [17], lack post processing data [5], or are bulky in size [20].

VII. CONCLUSION

A compact, complete and comprehensive imaging system is developed. The design of a modified side slotted Vivaldi antenna for microwave imaging applications has been quantified and characterized. The measurement results show that the antenna has a fractional bandwidth of approximately 127% from 1.54 to 7 GHz, with return loss$<$10 dB and a unidirectional radiation pattern, the maximum realized gain is 9.8 dBi and the radiation efficiency is approximately 92% over the bandwidth. To enhance the bandwidth, efficiency, and gain, the radiating patch and feed networks are optimized. The antenna is used for breast phantom measurements for detecting tumor cells inside a breast. An alternative stepper motor and microcontroller-based mechanical approach are developed for collecting data throughout the breast phantom. A custom-made transceiver, receiver, data acquisition model and image re-construction approach using Matlab have been developed. The remarkable variation in the scattered field is an important aspect for breast phantom scanners, and by analyzing these changes, conclusions can be drawn so that the system can localize unwanted tumor cells inside a human breast. The system is tested with an artificial breast phantom. The obtained performance of the imaging system supports its use for the early detection of unwanted tumors inside human breasts.

REFERENCES

[1] M. Kahar, A. Ray, D. Sarkar, and P. P. Sarkar, "An UWB microstrip monopole antenna for breast tumor detection," *Microw. Opt. Technol. Lett.*, vol. 57, no. 1, pp. 49–54, 2015.

[2] H. Zhang, "Microwave imaging for ultra-wideband antenna based cancer detection," Tech. Rep., 2015.

[3] H. Bahrami, E. Porter, A. Santorelli, B. Gosselin, M. Popovic, and L. A. Rusch, "Flexible sixteen monopole antenna array for microwave breast cancer detection," in *Proc. 36th Annu. Int. Conf. IEEE Eng. Med. Biol. Soc.*, Aug. 2014, pp. 3775–3778.

[4] Y. Zhang, W. Hong, C. Yu, Z. Q. Kuai, Y. D. Don, and J. Y. Zhou, "Planar ultrawideband antennas with multiple notched bands based on etched slots on the patch and/or split ring resonators on the feed line," *IEEE Trans. Antennas Propag.*, vol. 56, no. 9, pp. 3063–3068, Sep. 2008.

[5] M. Abbak, M. Çayören, and I. Akduman, "Microwave breast phantom measurements with a cavity-backed Vivaldi antenna," *IET Microw., Antennas Propag.*, vol. 8, no. 13, pp. 1127–1133, 2014.

[6] M. Chiappe and G. L. Gragnani, "Vivaldi antennas for microwave imaging: Theoretical analysis and design considerations," *IEEE Trans. Instrum. Meas.*, vol. 55, no. 6, pp. 1885–1891, Dec. 2006.

[7] A. T. Mobashsher, K. S. Bialkowski, A. M. Abbosh, and S. Crozier, "Design and experimental evaluation of a non-invasive microwave head imaging system for intracranial haemorrhage detection," *PLoS ONE*, vol. 11, no. 4, p. e0152351, 2016.

[8] S. A. AlShehri, S. Khatun, A. B. Jantan, R. S. A. R. Abdullah, R. Mahmud, and Z. Awang, "Experimental breast tumor detection using NN-based UWB imaging," *Prog. Electromagn. Res.*, vol. 111, no. 111, pp. 447–465, Jan. 2011.

[9] M. Koutsoupidou *et al.*, "Evaluation of a tumor detection microwave system with a realistic breast phantom," *Microw. Opt. Technol. Lett.*, vol. 59, no. 1, pp. 6–10, 2017.

[10] M. M. Islam, M. T. Islam, M. Samsuzzaman, M. R. I. Faruque, N. Misran, and M. F. Mansor, "A miniaturized antenna with negative index metamaterial based on modified SRR and CLS unit cell for UWB microwave imaging applications," *Materials*, vol. 8, no. 2, pp. 392–407, 2015.

[11] J. Zhang, E. C. Fear, and R. H. Johnston, "Cross-Vivaldi antenna for breast tumor detection," *Microw. Opt. Technol. Lett.*, vol. 51, no. 2, pp. 275–280, 2009.

[12] M. M. Islam, M. T. Islam, M. R. I. Faruque, M. Samsuzzaman, N. Misran, and H. Arshad, "Microwave imaging sensor using compact metamaterial UWB antenna with a high correlation factor," *Materials*, vol. 8, no. 8, pp. 4631–4651, 2015.

[13] H. M. Jafari, J. M. Deen, S. Hranilovic, and N. K. Nikolova, "Co-polarised and cross-polarised antenna arrays for breast, cancer detection," *IET Microw., Antennas Propag.*, vol. 1, no. 5, pp. 1055–1058, Oct. 2007.

[14] M. A. Alzabidi, M. A. Aldhaeebi, and I. Elshafiey, "Development of UWB Vivaldi antenna for microwave imaging," in *Proc. Saudi Int. Electron., Commun. Photon. Conf. (SIECPC)*, 2013, pp. 1–4.

[15] A. M. D. Oliveira, M. B. Perotoni, S. T. Kofuji, and J. F. Justo, "A palm tree antipodal Vivaldi antenna with exponential slot edge for improved radiation pattern," *IEEE Antennas Wireless Propag. Lett.*, vol. 14, pp. 1334–1337, 2015.

[16] I. T. Nassar and T. M. Weller, "A novel method for improving antipodal Vivaldi antenna performance," *IEEE Trans. Antennas Propag.*, vol. 63, no. 7, pp. 3321–3324, Jul. 2015.

[17] B. Wu, Y. Ji, and G. Fang, "Design and measurement of compact tapered slot antenna for UWB microwave imaging radar," in *Proc. 9th Int. Conf. Electron. Meas. Instrum. (ICEMI)*, 2009, pp. 2-226–2-229.

[18] S. H. He, W. Shan, C. Fan, Z. C. Mo, F. H. Yang, and J. H. Chen, "An improved Vivaldi antenna for vehicular wireless communication systems," *IEEE Antennas Wireless Propag. Lett.*, vol. 13, pp. 1505–1508, 2014.

[19] G. K. Pandey, H. Verma, and M. K. Meshram, "Compact antipodal Vivaldi antenna for UWB applications," *Electron. Lett.*, vol. 51, no. 4, pp. 308–310, 2015.

[20] S. Hu, W. B. Dou, and C. L. Law, "A tapered slot antenna with flat and high gain for ultra-wideband applications," *J. Electromagn. Waves Appl.*, vol. 23, pp. 723–728, Apr. 2009.

[21] E. C. Fear, P. M. Meaney, and M. A. Stuchly, "Microwaves for breast cancer detection?" *IEEE Potentials*, vol. 22, no. 1, pp. 12–18, Feb. 2003.

[22] H. Kanj and M. Popovic, "Miniaturized microstrip-fed 'Dark Eyes' antenna for near-field microwave sensing," *IEEE Antennas Wireless Propag. Lett.*, vol. 4, no. 1, pp. 397–401, 2005.

[23] B. J. Mohammed, A. M. Abbosh, and P. Sharpe, "Planar array of corrugated tapered slot antennas for ultrawideband biomedical microwave imaging system," *Int. J. RF Microw. Comput.-Aided Eng.*, vol. 23, no. 1, pp. 59–66, 2013.

[24] E. Guillanton, J. Y. Dauvignac, C. Pichot, and J. Cashman, "A new design tapered slot antenna for ultra-wideband applications," *Microw. Opt. Technol. Lett.*, vol. 19, no. 4, pp. 286–289, 1998.
[25] P. J. Gibson, "The Vivaldi aerial," in *Proc. 9th Eur. Microw. Conf.*, 1979, pp. 101–105.
[26] A. M. Abbosh, "Miniaturized microstrip-fed tapered-slot antenna with ultrawideband performance," *IEEE Antennas Wireless Propag. Lett.*, vol. 8, pp. 690–692, 2009.
[27] R. Natarajan *et al.*, "Modified antipodal Vivaldi antenna for ultra-wideband communications," *IET Microw., Antennas Propag.*, vol. 10, no. 4, pp. 401–405, 2016.
[28] C. A. Balanis, *Antenna Theory: Analysis and Design*. Hoboken, NJ, USA: Wiley, 2016.
[29] M. Z. Mahmud, S. Kibria, M. Samsuzzaman, N. Misran, and M. T. Islam, "A new high performance Hibiscus petal pattern monopole antenna for UWB applications," *Appl. Comput. Electromagn. Soc. J.*, vol. 31, no. 4, pp. 373–380, 2016.
[30] N. Ojaroudi, M. Ojaroudi, and Y. Ebazadeh, "UWB/omni-directional microstrip monopole antenna for microwave imaging applications," *Prog. Electromagn. Res. C*, vol. 47, no. 47, pp. 139–146, Mar. 2014.
[31] C. Sarkar, "Some parametric studies on Vivaldi antenna," *Int. J. u- e-Service, Sci. Technol.*, vol. 7, no. 4, pp. 323–328, 2014.
[32] L. Tianming, R. Yuping, and N. Zhongxia, "Analysis and design of UWB Vivaldi antenna," in *Proc. Int. Symp. Microw., Antenna, Propag. EMC Technol. Wireless Commun.*, Aug. 2007, pp. 579–581.
[33] K. R. Foster, J. L. Schepps, R. D. Stoy, and H. P. Schwan, "Dielectric properties of brain tissue between 0.01 and 10 GHz," *Phys. Med. Biol.*, vol. 24, no. 6, p. 1177, 1979.
[34] S. Gabriel, R. W. Lau, and C. Gabriel, "The dielectric properties of biological tissues: II. Measurements in the frequency range 10 Hz to 20 GHz," *Phys. Med. Biol.*, vol. 41, no. 11, p. 2251, 1996.
[35] J. Jossinet and M. Schmitt, "A review of parameters for the bioelectrical characterization of breast tissue," *Ann. New York Acad. Sci.*, vol. 873, pp. 30–41, Apr. 1999.
[36] W. T. Joines, Y. Zhang, C. Li, and R. L. Jirtle, "The measured electrical properties of normal and malignant human tissues from 50 to 900 MHz," *Med. Phys.*, vol. 21, pp. 547–550, Apr. 1994.
[37] S. Kibria, M. T. Islam, and B. Yatim, "New compact dual-band circularly polarized universal RFID reader antenna using ramped convergence particle swarm optimization," *IEEE Trans. Antennas Propag.*, vol. 62, no. 5, pp. 2795–2801, May 2014.

MOHAMMAD TARIQUL ISLAM (M'08–SM'13) was born in Dhaka, Bangladesh, in 1975. He is currently a Professor with the Department of Electrical, Electronic and Systems Engineering, Universiti Kebangsaan Malaysia (UKM), and also a Visiting Professor with the Kyushu Institute of Technology, Japan. He has authored about 350 research journal articles, nearly 165 conference articles, four research level books, and a few book chapters on various topics related to antennas, microwaves, and electromagnetic radiation analysis with 12 inventory patents filed. His publications have been cited 2700 times and his H-index is 28. He is currently involved in many research projects from the Malaysian Ministry of Science, Technology and Innovation and Ministry of Education. His research interests include communication antenna design, radio astronomy antennas, satellite antennas, and electromagnetic radiation analysis. He is a member of the Institute of Electronics, Information and Communication Engineers and the IET. He received several International Gold Medal awards, the Best Invention in Telecommunication Award, the Special Award from Vietnam for his research and innovation, and the Best Researcher Awards in 2010 and 2011 at UKM. He also received the Best Innovation Award in 2011 and the Best Research Group in ICT niche in 2014 by UKM. He was a recipient of the Publication Award from the Malaysian Space Agency in 2014, 2013, 2010, and 2009 and the Best Paper Presentation Award in 2012 International Symposium on Antennas and Propagation, Nagoya, Japan, and in 2015 in IconSpace. He currently serves as the Editor-in-Chief of the *International Journal of Electronics and Informatics* and also an Associate Editor of the *International Journal of Antenna and Propagation* and *Electronics Letter*.

MD. ZULFIKER MAHMUD was born in Rajshahi, Bangladesh, in 1984. He received the B.Sc. and M.Sc. degrees in computer science and engineering from Islamic University Kushtia, Bangladesh. He is currently pursuing the Ph.D. degree with the Universiti Kebangsaan Malaysia (UKM), Malaysia. He is also an Assistant Professor with the AIS Department, Jagannath University, Dhaka, Bangladesh. He is also a Graduate Research Assistant with the Department of Electrical, Electronic and Systems Engineering, UKM. His research interests include the microwave imaging, antenna design, satellite antennas, satellite communication, and wireless communication.

NORBAHIAH MISRAN received the B.Eng. degree in electrical, electronic and system engineering from Universiti Kebangsaan Malaysia (UKM) in 1999 and the Ph.D. degree from the Queen's University of Belfast, U.K., in 2004. She was a Tutor in 1999. She was a Lecturer in 2004 and an Associate Professor in 2009. She is currently a Professor with UKM. Her research interests include RF device design, particularly in broadband microstrip antennas, reconfigurable antennas, and reflect array antennas. She is also conducting some researches in engineering education field.

JUN-ICHI TAKADA (S'89–M'93–SM'11) received the B.E., M.E., and D.E. degrees in electrical and electronic engineering from the Tokyo Institute of Technology, Tokyo, Japan, in 1987, 1989, and 1992, respectively. From 1992 to 1994, he was a Research Associate with Chiba University, Chiba, Japan. From 1994 to 2006, he was an Associate Professor with the Tokyo Institute of Technology, where he has been a Professor since 2006. From 2003 to 2007, he was a Researcher with the National Institute of Information and Communications Technology, Kyoto, Japan. His research interests include radio-wave propagation and channel modeling for mobile and short range wireless systems, regulatory issues of spectrum sharing, and ICT applications for international development. He has been appointed as an IEICE Fellow in 2012. He received the Achievement Award of IEICE in 2008. From 2007 to 2010, he was a Co-Chair of the Special Interest Group on Body Communications, EU COST Action 2100.

MENGU CHO received the B.S. and M.S. degrees from The University of Tokyo, Tokyo, Japan, in 1985 and 1987, respectively, and the Ph.D. degree from the Department of Aeronautics/Astronautics, Massachusetts Institute of Technology, Cambridge, MA, USA, in 1992. From 1992 to 1995, he was a Research Associate with Kobe University, Kobe, Japan. From 1995 to 1996, he was a Teaching Associate with International Space University, Illkirch-Graffenstaden, France. Since 1996, he has been with the Kyushu Institute of Technology (KIT), Kitakyushu, Japan, where he was an Assistant Professor in 1996 and an Associate Professor in 1997. Since 2004, He has been a Professor and the Director of the Laboratory of Spacecraft Environment Interaction Engineering, KIT. Since 2010, he has been with the Department of Applied Science for Integrated System Engineering. He has authored or co-authored over 140 papers in peer reviewed journals. His research interests include spacecraft environmental interaction, particularly spacecraft charging and nano-satellite reliability.